Communication

Synthesis and Characterization of Manganese-Doped Silicon Nanoparticles: Bifunctional Paramagnetic-Optical Nanomaterial

Xiaoming Zhang, Marcin Brynda, R. David Britt, Elizabeth C. Carroll, Delmar S. Larsen, Angelique Y. Louie, and Susan M. Kauzlarich

J. Am. Chem. Soc., **2007**, 129 (35), 10668-10669• DOI: 10.1021/ja074144q • Publication Date (Web): 11 August 2007

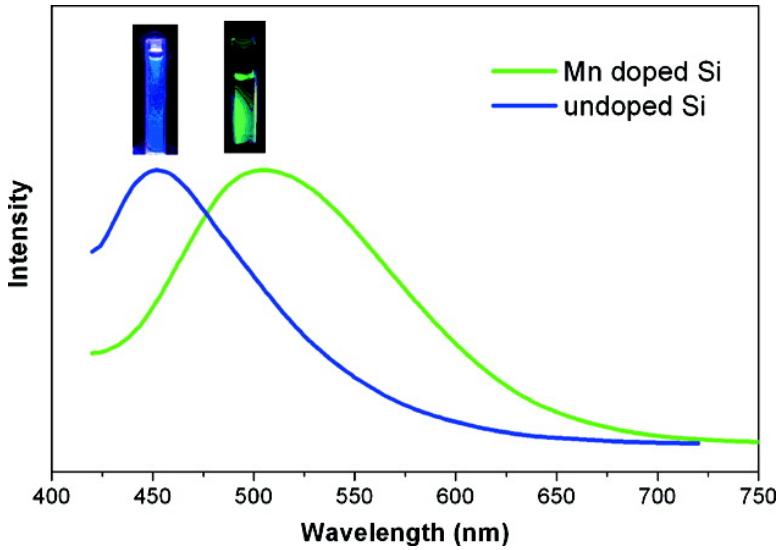

More About This Article

Additional resources and features associated with this article are available within the HTML version:

- Supporting Information
- Links to the 4 articles that cite this article, as of the time of this article download
- Access to high resolution figures
- Links to articles and content related to this article
- Copyright permission to reproduce figures and/or text from this article

View the Full Text HTML

J|A|C|S
COMMUNICATIONS

Published on Web 08/11/2007

Synthesis and Characterization of Manganese-Doped Silicon Nanoparticles: Bifunctional Paramagnetic-Optical Nanomaterial

Xiaoming Zhang,[†] Marcin Brynda,[‡] R. David Britt,[‡] Elizabeth C. Carroll,[‡] Delmar S. Larsen,[‡] Angelique Y. Louie,[†] and Susan M. Kauzlarich*[,‡]

Department of Biomedical Engineering and Department of Chemistry, University of California, Davis, California 95616

Received June 7, 2007; E-mail: smkauzlarich@ucdavis.edu

Multifunctional nanomaterials are multiphase nanostructures with combined functionality such as detection by multiple imaging modalities, or detection and therapy. These nanomaterials possess combinations of properties that do not exist in single-phase materials. Nanoparticles, in particular, have potential for multimodal biological applications by the addition of functionality to augment their luminescence.[1−3] Nanoparticles have intense visible luminescence because of quantum confinement, and the color can be tuned throughout the visible spectrum by changing the particle size.[4,5] Because of their biocompatibility, high photoluminescence quantum efficiency, and stability against photobleaching, silicon nanoparticles are expected to be an ideal candidate in many biological assays and fluorescence imaging techniques.[6−8] The addition of paramagnetism to silicon nanoparticles would allow combinations of optical detection with magnetic resonance imaging detection or magnetic separation.

An effective method for manipulating the physical properties of semiconductors involves impurity doping.[9] Groups II−VI semiconductor quantum dots can be doped with metal ions that have energy states within the band gap. As a result, light emission from these introduced trap states can be observed.[10] The advantage of this approach is that color can be controlled by the nature of the dopant, which allows for similar sized quantum dots with a full spectrum of colors. Doped nanomaterials provide the possibility for enhanced, multimodal functionality in contrast to their single-component counterparts.[11] Recently, Mn doped group IV semiconductors have attracted much attention both in experiment and theory.[12−14]

In this Communication, we describe our syntheses of Mn doped Si nanoparticles and characterize the optical and magnetic properties of the system. Recently, a solution route has been used to produce macroscopic amounts of either amorphous or crystalline hydrogen terminated Si nanoparticles in our laboratory.[15,16] Herein, Mn doped Zintl salts ($NaSi_{1-x}Mn_x$, $x = 0.05$, 0.1, 0.15) were prepared as precursors, followed by the reaction with ammonium bromide to make hydrogen capped nanocomposites.

$$NaSi_{1-x}Mn_x + NH_4Br \rightarrow Si_{1-x}Mn_x - H + NH_3 + NaBr \quad (1)$$

The hydride-capped Mn doped silicon nanoparticles can be modified further via a hydrosilylation process to form chemically robust Si−C bonds on the surface and to protect the silicon particles from oxidation.[17,18] The nanoparticles described herein were capped with octyne to form organic soluble nanoparticles.

Figure 1A shows representative TEM image of 5% Mn doped Si nanoparticles collected on a carbon TEM grid. The percentage

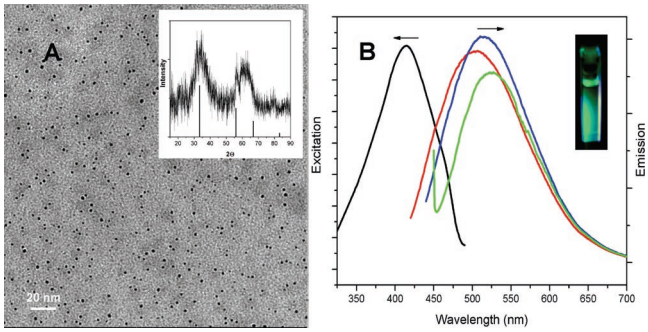

Figure 1. (A) TEM image of 5% Mn-doped Si nanoparticles. Inset is XRD pattern of Mn-doped silicon nanoparticles. The lines indicate the X-ray diffraction peak position for diamond structure silicon. (B) Excitation spectra (black) and room-temperature PL spectra of Si nanoparticles in chloroform at different excitation wavelengths: 400 nm (red), 420 nm (blue), and 440 nm (green). The inset shows fluorescence from a cuvette of Mn-doped Si nanoparticles when excited with a handheld UV lamp.

of Mn in the Si nanoparticle sample was confirmed by elemental analysis with a molar ratio of Si/Mn of 18.2:1, consistent with 5% Mn doped Si nanoparticles, and all the characterization described herein are on samples with nominally 5% Mn doping. The average diameter of Si nanoparticles is 4.2 ± 0.9 nm based on a survey of 530 particles from different regions of the grid. This result is similar to that for undoped Si nanoparticles prepared by this same method.[15]

The inset of Figure 1A shows the X-ray powder diffraction pattern of the obtained Mn doped Si nanoparticles. The diffraction pattern shows two broad diffraction peaks at approximately 33° and 60°, consistent with observations for amorphous silicon.[16,19] The narrow peaks at 32° and 56° could correspond to the (111) and (220) reflections of crystalline silicon. The diffraction pattern can be interpreted as due to mainly amorphous Si.[16] No diffraction due to Mn and MnO_x phases are observed, suggesting that Mn is incorporated into the Si nanoparticles.

Photoluminescence (PL) spectra (excitation and emission) were used to investigate the optical properties of the Mn-doped silicon nanoparticles in chloroform (Figure 1B). The excitation spectrum (black curve) shows that monitored at excitation wavelength 510 nm, the Mn doped Si nanoparticle sample gave the strongest peak when excited at 420 nm. The emission spectra show a relatively narrow region of intense luminescence with maximum intensity from 490 to 520 nm, with excitation from 380 to 440 nm. The maximum intensity emission spectrum is centered at 510 nm with an excitation wavelength of 420 nm. Compared to the undoped Si nanoparticles,[15] there is an obvious red shift from 430 to 520 nm. Changes in the excitation wavelength excited different size populations of nanoparticles, resulting in the varying emission wavelengths observed. Quantum yields of up to 16% in chloroform were obtained relative to the standard fluorescein solution[20] for the Mn-doped Si

[†] Department of Biomedical Engineering.
[‡] Department of Chemistry.

10.1021/ja074144q CCC: $37.00

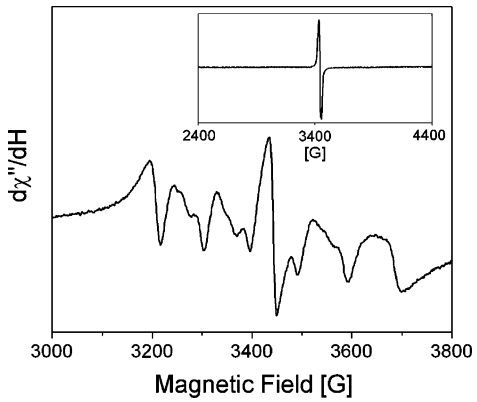

Figure 2. EPR spectrum of the Mn^{2+} doped Si nanoparticles. The inset shows EPR spectrum of the undoped Si nanoparticles.

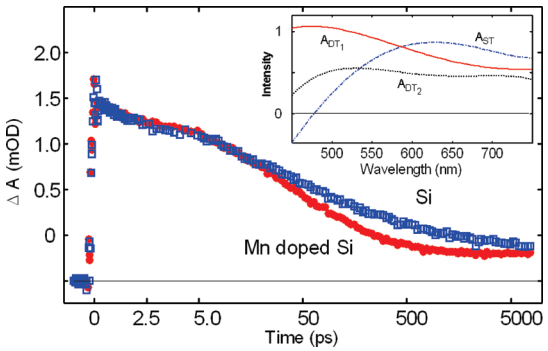

Figure 3. Transient absorption spectroscopy probed at 525 nm in Mn-doped Si and undoped Si nanoparticles. The inset shows global analysis that was used to determine species associated spectra for three electron populations in shallow traps (ST) and deep traps (DT1 and DT2).

sample, lower than that reported for undoped Si prepared in the same manner (18%).[15] With larger amounts of Mn, the quantum yield decreased significantly.

Electron paramagnetic resonance (EPR) measurements (Figure 2) were used to confirm the presence of Mn^{2+} in the Si nanoparticles. The EPR spectrum of the undoped samples (inset Figure 2) shows a sharp signal at $g = 2.0$, attributed to dangling bonds in the Si nanoparticles.[21] In addition to the $g = 2.0$ signal, the Mn-doped sample exhibits a six-line spectrum, arising from the hyperfine interaction with the ^{55}Mn nuclear spin ($I = {}^5/_2$).[22] The observed hyperfine splitting is 96 G and is similar to the hyperfine splitting observed for Mn^{2+} ions isolated on the surface of Si rather than in the interior.[23] To rule out the possible presence of the Mn^{2+} ions simply physisorbed on the Si surface, an additional set of samples were prepared by successive purification (washed four times with a chloroform/methanol mixture) followed by ligand exchange with pyridine to remove Mn^{2+} from the surface of the particles.[11] The corresponding EPR spectra are almost identical to the one obtained with the nonwashed samples, and the Mn hyperfine splitting value remains the same, suggesting that Mn^{2+} is covalently bound to the surface or near the surface of the nanoparticle (Supporting Information). The presence of Mn^{2+} near or at the surface would be optimal for MRI applications.

Additional evidence for Mn doped into the nanoparticles can be provided by transient absorption (TA) spectroscopy. TA data show that the excited-state dynamics of the 5% Mn doped Si nanoparticles differs distinctly from undoped Si nanoparticles (Figure 3). At least two trapped electronic populations can be distinguished spectroscopically in the undoped Si nanoparticles (inset, Figure 3). The population associated with higher energy electron trap states decays ~20% more quickly in the Mn-doped Si nanoparticles, suggesting that photogenerated excitons have additional relaxation paths. Similarly faster trapped electron relaxation has been observed in Er^{3+}-doped Si nanocrystals.[24] A ns plateau in absorption also indicates a longer lived charge separation in the Mn doped Si nanoparticles. One explanation for the differences in dynamics is a terminal migration of charge carriers from Si traps to Mn states. The red-shifted emission spectrum of Mn-doped Si indicates recombination from trap states that are on average >0.1 eV lower in energy than trap states in undoped Si. These states are likely associated with Mn^{2+}, from which radiative recombination is inhibited both by a highly localized electron and because the d−d transition is not spin allowed.[25] Because radiative trap sites in Si nanoparticles are attributed to nonquantized surface states,[26] electron transfer from deep Si traps suggests that Mn^{2+} is coupled to the Si surface.

Acknowledgment. This work was supported by the NIH (Grant HL081108-01).

Supporting Information Available: Experimental procedures and characterization of Mn^{2+} doped silicon, an EPR spectrum of the Mn^{2+} doped Si nanoparticles followed by successive purification, and the FT-IR spectrum. This material is available free of charge via the Internet at http://pubs.acs.org.

References

(1) Huh, Y.-M.; Jun, Y.-w.; Song, H.-T.; Kim, S.; Choi, J.-s.; Lee, J.-H.; Yoon, S.; Kim, K.-S.; Shin, J.-S.; Suh, J.-S.; Cheon, J. *J. Am. Chem. Soc.* **2005**, *127*, 12387−12391.
(2) Santra, S.; Yang, H.; Holloway, P. H.; Stanley, J. T.; Mericle, R. A. *J. Am. Chem. Soc.* **2005**, *127*, 1656−1657.
(3) Michalet, X.; Pinaud, F. F.; Bentolila, L. A.; Tsay, J. M.; Doose, S.; Li, J. J.; Sundaresan, G.; Wu, A. M.; Gambhir, S. S.; Weiss, S. *Science* **2005**, *307*, 538−544.
(4) Canham, L. T. *Appl. Phys. Lett.* **1990**, *57*, 1046−1048.
(5) Veinot, J. G. C. *Chem. Commun.* **2006**, 4160−4168.
(6) Li, Z. F.; Ruckenstein, E. *Nano Lett.* **2004**, *4*, 1463−1467.
(7) Wang, L.; Reipa, V.; Blasic, J. *Bioconjugate Chem.* **2004**, *15*, 409−412.
(8) Buriak, J. M. *Philos. Trans. R. Soc. London, Ser. A* **2006**, *364*, 217−225.
(9) Shi, W.; Zeng, H.; Sahoo, Y.; Ohulchanskyy, T. Y.; Ding, Y.; Wang, Z. L.; Swihart, M.; Prasad, P. N. *Nano Lett.* **2006**, *6*, 875−881.
(10) Murphy, C. J.; Coffer, J. L. *Appl. Spectrosc.* **2002**, *56*, 16A−27A.
(11) Wang, S.; Jarrett, B. R.; Kauzlarich, S. M.; Louie, A. Y. *J. Am. Chem. Soc.* **2007**, *129*, 3848−3856.
(12) Yoon, I. T.; Park, C. J.; Kang, T. W. *J. Magn. Magn. Mater.* **2007**, *311*, 693−696.
(13) Li, A. P.; Shen, J.; Thompson, J. R.; Weitering, H. H. *Appl. Phys. Lett.* **2005**, *86*, 152507/1−152507/3.
(14) Jamet, M.; Barski, A.; Devillers, T.; Poydenot, V.; Dujardin, R.; Bayle-Guillemaud, P.; Rothman, J.; Bellet-Amalric, E.; Marty, A.; Cibert, J.; Mattana, R.; Tatarenko, S. *Nat. Mater.* **2006**, *5*, 653−659.
(15) Zhang, X.; Neiner, D.; Wang, S.; Louie, A. Y.; Kauzlarich, S. M. *Nanotechnology* **2007**, *18*, 095601.
(16) Neiner, D.; Chiu, H. W.; Kauzlarich, S. M. *J. Am. Chem. Soc.* **2006**, *128*, 11016−11017.
(17) Liao, Y.-C.; Roberts, J. T. *J. Am. Chem. Soc.* **2006**, *128*, 9061−9065.
(18) Liu, S. M.; Yang, Y.; Sato, S.; Kimura, K. *Chem. Mater.* **2006**, *18*, 637−642.
(19) Kapaklis, V.; Politis, C.; Poulopoulos, P.; Schweiss, P. *Appl. Phys. Lett.* **2005**, *87*, 123114/1−123114/3.
(20) Brannon, J. H.; Magde, D. *J. Phys. Chem.* **1978**, *82*, 705−709.
(21) Arul Dhas, N.; Raj, C. P.; Gedanken, A. *Chem. Mater.* **1998**, *10*, 3278−3281.
(22) Norris, D. J.; Yao, N.; Charnock, F. T.; Kennedy, T. A. *Nano Lett.* **2001**, *1*, 3−7.
(23) Ludwig, G. W.; Woodburg, H. H.; Carlson, R. O. *J. Phys. Chem. Solids* **1959**, *8*, 490−492.
(24) Samia, A. C. S.; Lou, Y.; Burda, C.; Senter, R. A.; Coffer, J. L. *J. Chem. Phys.* **2004**, *120*, 8716−8723.
(25) Smith, B. A.; Zhang, J. Z.; Joly, A.; Liu, J. *Phys. Rev. B* **2000**, *62*, 2021−2028.
(26) Klimov, V. I.; Schwarz, C. J.; McBranch, D. W.; White, C. W. *Appl. Phys. Lett.* **1998**, *73*, 2603−2605.

JA074144Q